



Theoretical and experimental study towards a nanogap dielectric biosensor

Mingqiang Yi*, Ki-Hun Jeong, Luke P. Lee

*Department of Bioengineering, Berkeley Sensor and Actuator Center, University of California,
1822 Francisco St., 18, Berkeley, CA 94720, USA*

Received 17 February 2004; received in revised form 30 April 2004; accepted 5 May 2004

Abstract

Theoretical and experimental studies of nanogap capacitors as potential label free biosensors are presented. The nanogap device is capable of detecting the existence of single stranded DNA (ssDNA) oligonucleotides (20-mer) in 100 nM aqueous solutions using a 20 nm gap of 1.2 pL in volume. While the dielectric properties of DNA solution have been widely investigated, early approaches are limited at low frequency by the parasitic noise due to the electrical double layer (EDL) impedance. Nanogap electrodes have the potential to serve as biomolecular junctions because their size (5–100 nm) minimizes electrode polarization effects regardless of frequency. In this paper, we modeled the effects of the EDL interaction between two parallel nanogap electrodes by solving the Poisson–Boltzmann (PB) equation for equilibrium state. When the gap size is smaller than the EDL thickness, the dependence of the nanogap capacitance on the ionic strength is insignificant. This is critical in using the capacitance change as an indicator of the existence of target molecules. The predicted capacitance of nanogaps filled with various ionic strength electrolytes was in quantitative agreement with the experimental measurements. The various concentrations of the target molecules in nanogap sensor were characterized. A capacitance change of a 20 nm × (10)1.5 μm × 4 mm gap from 3.5 to 4.1 nF at 200 Hz was recorded between deionized water (DI) and 100 nM ssDNA solution (about 70,000 molecules inside the gap for equilibrium state). © 2004 Elsevier B.V. All rights reserved.

Keywords: Nanogap; Poisson–Boltzmann equation; Electrical double layer; Effective permittivity; Dielectric relaxation

1. Introduction

Biosensor technologies have been widely studied. They have been based on electrochemical (Palecek et al., 1998; Marrazza et al., 1999), optical (Piunno et al., 1994), mass sensitive (Okahata et al., 1998), and acoustic wave transducers (Zhang et al., 1998). Recently, nanogap capacitors for direct electrical DNA detection without labeling like fluorescent, electrochemical intercalate, magnetic, nanoparticles etc have been fabricated and used (Lee et al., 2002; Sebaek et al., 2003). The dielectric detection mechanism (capacitance change) of a nanogap sensor promises fast and direct in situ monitoring of DNA hybridization without a time consuming DNA labeling procedure.

The dielectric properties of molecules depend on electron transfer, atomic bonds, and the large-scale molecular structure. The characteristic time scales range from 10⁻¹² s for

electrons, 10⁻⁹ s for atomic bonds, to 10⁻³ s for molecular structures. Therefore, when an oscillatory field perturbs molecules, they respond differently depending on the frequency. The low frequency response indicates the large-scale molecular structure changes like the conformation changes of DNA during hybridization from single stranded DNA (ssDNA) to double stranded DNA. The dielectric response of DNA in solution has been widely studied (Saif et al., 1991; Mandel, 1977; van der Touw and Mandel, 1974; Takashima, 1963, 1966, 1967; Baker-Jarvis et al., 1998). Dielectric relaxation of DNA solution occurs at least at three different frequency regions: α (a few kilohertz or lower), β (roughly from 1 MHz to 1 GHz), and γ (above 1 GHz). Among them, α relaxation has a large dielectric increment which is dependent on the length of the DNA molecule. And it reflects the migration of counter ions over the entire dimension of the DNA molecule. This close relationship between α relaxation and the EDL makes it difficult to do dielectric measurements at low frequency. Early dielectric spectroscopy of DNA solution was limited at low frequency due to the

* Corresponding author. Tel.: +1 510 642 5855; fax: +1 510 642 5835.
E-mail address: lp1ee@socrates.berkeley.edu (M. Yi).

noise from EDL impedance, which dominates the measured capacitance.

The EDL impedance is due to the accumulation of counter ions near the electrode surface, which becomes charged when in contact with an electrolyte (Hunter, 1993). The distribution of electrolyte ions in the vicinity of a charged surface was first predicted by Gouy (1910) and Chapman (1913) by assuming the Boltzmann distribution for ions and ion interaction with a mean potential governed by Poisson equation, i.e. Poisson–Boltzmann (PB) equation. The basic feature is the build up of an electrical double layer adjacent to the electrode surface. In the case of the nanogap, all EDLs interact with each other due to the space confinement. We expect this EDL interaction would minimize the contribution of EDL on measured capacitance. To quantify this effect, we need to solve the electrical potential and ion distributions within nanogap, i.e. the PB equation since the PB equation can still predict the electrostatic interaction of close surfaces in water when two electrode surfaces come close (Biesheuvel, 2001; Basu and Sharma, 1994; Zhmud et al., 1998). Then we calculated the capacitance of the gap when filled with various ionic strength electrolytes. We compared these theoretical results with the experimental measurements on a 22 nm gap. The measured capacitance appeared barely dependent on the ionic strength provided the gap size was smaller than the EDL thickness. This finding is very important when the nanogap is used to detect target molecules in the electrolytes. The capacitance of another 22 nm gap filled with target molecule aqueous solution was measured. The

capacitance of the gap was twice of that for DI water filled gap at 200 Hz, showing the existence of DNA. A 30% capacitance change at frequency 200 Hz was also observed due to the DNA concentration change. Further, in using a $20 \text{ nm} \times (10)1.5 \mu\text{m} \times 4 \text{ mm}$ gap (about 1.2 pl in volume) to detect the existence of target molecule, the capacitance filled with 100 nM target molecular solution was about 4.1 nF while the de-ionized water (DI) filled gap had a capacitance of 3.5 nF.

2. Theory

We focus on the essential feature of a nanogap: gap size, which is comparable to the electrical double layer thickness. As shown in Fig. 1c, the nanogap sensor consisted of two parallel electrodes. The distance between the two electrodes was $2L$. The thickness of the electrical double layer is the reciprocal of the Debye–Hückel parameter, κ (Hunter, 1993). $\kappa = 3.288\sqrt{I}$ at 298 K in water, where I is the ionic strength of the electrolytes. For example, $\kappa^{-1} = 960 \text{ nm}$ when $I = 10^{-7} \text{ M}$ and $\kappa^{-1} = 9.6 \text{ nm}$ when $I = 10^{-3} \text{ M}$. For large separations, one has $\kappa L = \infty$. However, within a nanogap, κL is a finite number that we defined as the size of the nanogap, S_n . We set the origin of the one-dimensional coordinate (x) in the middle of the nanogap and the direction perpendicular to the electrode surface. Taking advantage of the symmetry, we solved the problem at $0 \leq x \leq L$.

Assuming thermodynamically ideal systems, the Boltzmann equation gives the distribution of ion species i , C_i , at

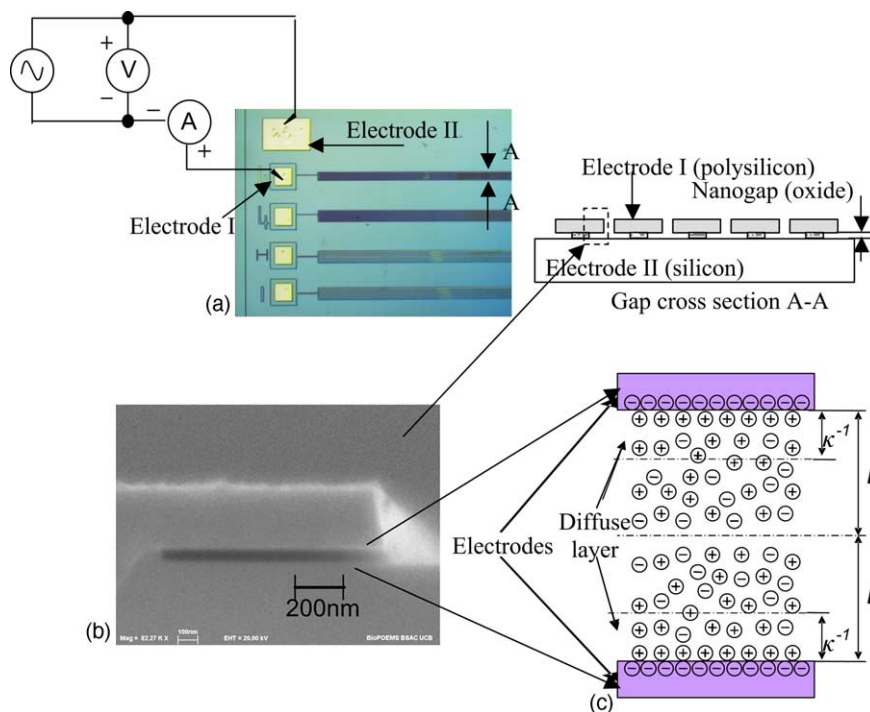


Fig. 1. Experimental set-up measuring nanogap capacitance. (a) Sketch of a two-wire impedance measurement set-up connected to the electrodes of the nanogap; (b) SEM of a nanogap fabricated using same masks for the tested nanogap; (c) nanogap filled with electrolytes (two length scales, gap size L and electrical double layer thickness κ^{-1} , exist).

equilibrium

$$C_i = C_{i0} \exp\left(\frac{z_i e \phi}{k_B T}\right) \quad (1)$$

where z_i is the valence of the species, e is the electron charge (1.6022×10^{-19} C), k_B is the Boltzmann constant (1.3807×10^{-23} J/K), T is the temperature (assuming 298 K), ϕ is the electrical potential, and C_{i0} is the ion species concentration at $\phi = 0$.

The space charge density, ρ (C/m³), is obtained by adding charges from all ion species. To simplify the algebra, we set $z_i = z_+ = -z_- = z$ so that the analysis was limited to symmetrical $z:z$ valent electrolytes. This is not a serious restriction because in most situations the behavior is determined overwhelmingly by the ions of sign opposite to that of the surface. We also assumed $C_{+0} = C_{-0} = C_0$, then the space charge is

$$\rho = -2C_0 z e \sinh \frac{ze\phi}{k_B T} \quad (2)$$

Assuming constant permittivity, ϵ , and neglecting polarization effects, the electrical potential field (ϕ) is governed by the Poisson equation. We non-dimensionalized the problem with electrical potential scale $V = k_B T / ze$, which is 25.68 mV when $z = 1$ and $T = 298$ K, and length scale L , i.e. set $\phi = (k_B T / ze)\Phi$ and $x = LX$. We then multiplied both sides of the Poisson equation by $2(d\Phi/dX)$, and integrated from 0 to X . Applying the symmetry condition, $(d\Phi/dx)|_{X=0} = 0$, we had

$$\left(\frac{d\Phi}{dX}\right)^2 = 4S_n^2 [\cosh\Phi - \cosh\Phi(0)] \quad (3)$$

where $S_n^2 = \kappa^2 L^2$ and $\kappa^2 = C_0 z^2 e^2 / \epsilon k_B T$ and κ is the Debye–Hückel parameter.

To obtain another boundary condition, we assumed that the charge on the electrode surface, σ , should balance the charge within the nanogap, i.e.

$$\sigma = 2C_0 z e L \int_{x=0}^1 \sinh\Phi dX \quad (4)$$

For positive X pointing from the solution to the surface, the Gauss law relates the surface charge to the electrical field intensity, i.e. $d\phi/dX = \sigma/\epsilon$ on the electrode surface. So we had

$$\frac{d\Phi}{dX} = 2S \int_{x=0}^1 \sinh\Phi dX \quad \text{at } X = 1 \quad (5)$$

The electrical potential field was obtained by numerically solving Eq. (3), satisfying the boundary condition (5). Then the capacitance of the nanogap, C (F/m²), was calculated as $\sigma/(2(\phi(L) - \phi(0)))$ i.e.

$$C = \frac{\epsilon}{L} S_n^2 \int_{x=0}^1 \sinh\Phi dX \frac{1}{\Phi(1) - \Phi(0)} \quad (6)$$

We defined the effective permittivity, ϵ_e , of the nanogap so that the capacitance of the nanogap was $C = \epsilon_e/2L$. Comparing Eq. (6), we had

$$\frac{\epsilon_e}{\epsilon} = 2S_n^2 \int_{x=0}^1 \sinh\Phi dX \frac{1}{\Phi(1) - \Phi(0)} \quad (7)$$

3. Experimental method

The nanogap dielectric biosensors consisted of a capacitor between two parallel polysilicon electrodes fabricated using standard CMOS technology. The distance between two electrodes can be controlled from 5 to 100 nm. The capacitance of the nanogap indicates the permittivity of the medium filling the gap. The nanogap sensor, schematically shown in Fig. 1a, features a horizontal air nanogap bordered at the top by a polysilicon layer and at the bottom by a doped silicon layer. This gap is created by selective etching of the thermally grown oxide between the polysilicon and doped silicon layers. The thermally grown oxide layer defines the width of nanogap dielectric sensor. Fig. 1b depicts the SEM photo of a 60 nm gap.

The Novocontrol Alpha-N dielectric analyzer connected to the probe station employed a two-wire impedance measurement set-up. We made contact to the sensor at two points: (1) to a gold pad that is connected to the doped polysilicon layer, and (2) to another gold pad that is connected to the doped silicon substrate, as shown in Fig. 1a. For our experiments, we set the a.c. generator amplitude to 30 mV RMS with 0 V d.c. bias. We took measurements from 1 MHz down to 1 Hz with a frequency spacing factor of 1.5. The WinData software controlled and recorded the capacitance measurements through a GPIB interface. Each sweep took approximately 1 min to acquire. At each frequency, we recorded the permittivity, ϵ , the parallel capacitance, C_p , and the loss tangent, $\tan \delta$. The loss tangent was a measure of the conductivity of the sensor under test and is used to monitor the performance of the sensor. A loss tangent higher than 100 implied that the sensor's conductance was too high and no longer behaved as a capacitor. In this case, it became difficult to accurately measure the series capacitance, and hence, the permittivity, of the sample.

We verified proper contact and proper functioning of the sensor by measuring the dielectric spectrum with just air in the gap. The permittivity was derived from the capacitance ($\epsilon = C(L/A)$). For each sample, we repeated the measurement three times and the variations of the measured capacitance were within 3%.

We prepared various ionic strength solutions by diluting phosphate-buffered saline or PBS buffer solution (Invitrogen Corporation, Grand Island, NY) in DI water. The target molecule (single stranded DNA, 5'-TGCA-GTTTTCCAGCAATGAG, purchased from Alpha DNA, Montreal, Quebec, Canada) solution was prepared by

dissolving and diluting the DNA in DI water until the desired concentration was achieved.

We prepared the sensor to hold the fluid samples by placing a poly-dimethylsiloxane (PDMS) well on top of the wafer. The PDMS well was approximately $7\text{ mm} \times 7\text{ mm} \times 1\text{ mm}$ with a 4 mm diameter hole in the middle to act as a solution reservoir. The PDMS well was placed to maximize the sensor area exposed to the solution while keeping the sensor contact points dry and just outside the well.

3.1. Various ionic strength electrolytes or various concentration DNA solutions

We used the protocol below to measure the response of the nanogap sensor to de-ionized water and varying concentrations of buffer or DNA solution. The order of introducing the solutions were from DI to monotonically increasing concentrations of buffer or DNA solution in order to avoid any errors due to fluid leftover from a previously higher concentration. First, $40\ \mu\text{l}$ of fluid were pipette into the PDMS well; 1 min after placing fluid, dielectric spectrum was measured, then the measurements were repeated twice; the fluid was removed from the well using a small strip of lint-free absorbent paper.

The time from the removal of the fluid to the introduction of new fluid was 2 min. Because of the small amount of fluid sample and lack of a flow-thru set-up, measurement error due to sample evaporation was possible. We estimated that its contribution was less than 1% over the frequency range of interest. We obtained this estimation by comparing the difference in the dielectric spectrum between 40 and $20\ \mu\text{l}$ of sample fluid in the PDMS well.

3.2. Evaporation of DNA solutions

In another way to test the response of the nanogap sensor to DNA solutions of various concentrations, $25\ \mu\text{l}$ of $0.5\ \mu\text{M}$ DNA solution was initially pipetted into the PDMS well. The well was open to the atmosphere and the water slowly evaporated. The DNA concentration therefore changed constantly, but slowly, maintaining uniform DNA concentration within the sample solution through diffusion. The dielectric spectrum of the sample was measured as a function of time. After 170 min, the capacitance change due to the water evaporation was very slow. We subsequently baked the device at 120°C for 10 min to dry the device completely and measured its capacitance. If the capacitance of the dried device was higher than its capacitance filled with air before adding the DNA solution, we also effectively verified that DNA did enter the gap.

4. Results and discussion

Fig. 2 depicts the theoretical static electrical potential distribution within various size nanogaps. When the gap size

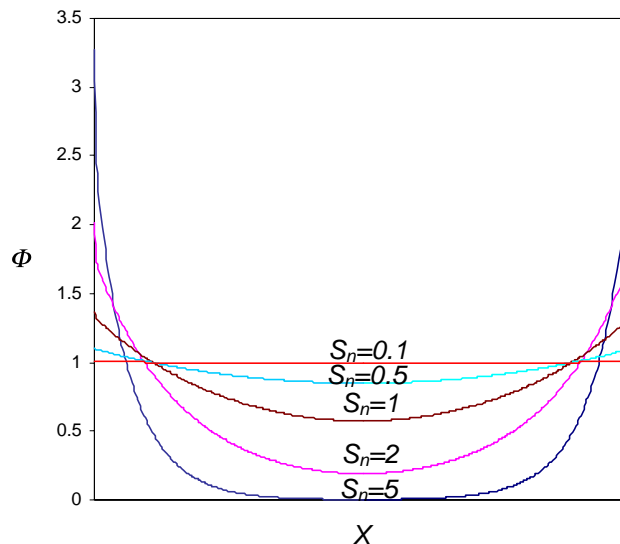


Fig. 2. Electrical potential distribution within nanogaps of various sizes. The potential in the middle of the gap decreases as the gap size increases while the potential on the electrode surfaces increases.

was big ($S_n = 5$), our solution recovered the boundary condition for bulk flow, i.e. $\Phi = 0$ in the middle of the gap. When the gap size (L) was comparable to or smaller than the electrical double layer thickness (κ^{-1}) ($S_n \leq 1$), decreasing ionic strength (S_n decreased) decreased the potential differences between the electrode surfaces and the middle of the gap, hence increasing the capacitance (as the ratio between the accumulated charge and the potential difference). At the same time, the accumulated charge also decreased, thus decreasing the parasitic capacitance by the EDL. These two competing effects almost canceled each other when $S_n \leq 1$ (ϵ_e/ϵ is within 2.3 ± 0.05), with the result that the effective permittivity is not significantly influenced by the ionic strength or gap size. This is beneficial factor for using nanogap capacitor to detect the change in permittivity when the target molecules were introduced into the electrolytes. To verify our solution, we measured the capacitance of 22 nm gap filled with different ionic strength electrolytes (10^{-7} to 10^{-2} M , corresponding to $\kappa^{-1} = 960\text{--}3\text{ nm}$). Fig. 3 shows the measured permittivity as a function of the frequency at various ionic strengths (I). The measurements were done at a series of increasing electrolyte ionic strength. When the ionic strength was increased from 10^{-7} ($\kappa^{-1} = 960\text{ nm}$) to 10^{-4} M ($\kappa^{-1} = 30\text{ nm}$), the measured permittivity was slightly decreased (Fig. 3a). As the ionic strength was further increased (Fig. 3b), the measured permittivity started increasing. This trend confirmed the existence of a minimum capacitance as the ionic strength changes from 10^{-7} to 10^{-2} M ($\kappa^{-1} = 3\text{ nm}$), which was estimated to be $4 \times 10^{-4}\text{ M}$ ($S_n = 0.72$). The experiments were repeated three times to confirm the observation. Fig. 4 depicts ϵ' as a function of the ionic strength together with the experimental measurements in a 22 nm gap for different ionic strength

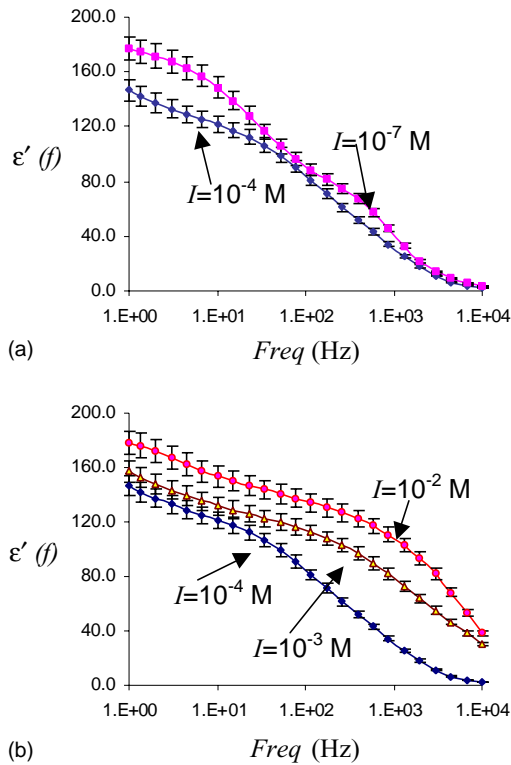


Fig. 3. The measured permittivity as a function of the frequency for a 22 nm gap filled with various ionic strength electrolytes. (a) The measured permittivity was slightly decreased as the ionic strength increases from 10^{-7} ($\kappa^{-1} = 960$ nm) to 10^{-4} M ($\kappa^{-1} = 30$ nm); (b) the measured permittivity started increasing as the ionic strength was further increased.

electrolytes (10^{-7} – 10^{-2} M, corresponding to $\kappa^{-1} = 960$ – 3 nm). The measured permittivity showed similar dependence on the ionic strength when the frequency equals 1, 10, 116, or 1317 Hz. The measured permittivity changed

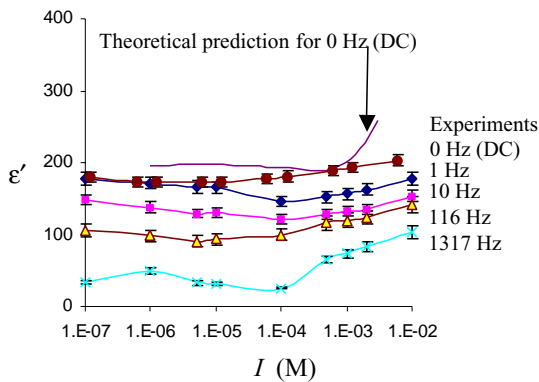


Fig. 4. Calculated permittivity as a function of the ionic strength in nanogaps of various sizes together with the experimental measurements in a 22 nm gap for different ionic strength electrolytes (10^{-7} – 10^{-2} M, corresponding to $\kappa^{-1} = 960$ – 3 nm). The measured permittivity showed similar dependence on the ionic strength for DC and when the frequency equaled 1, 10, 116, or 1317 Hz. ϵ_c/ϵ is within 2.3 ± 0.05 when $S_n = \kappa L \leq 1$.

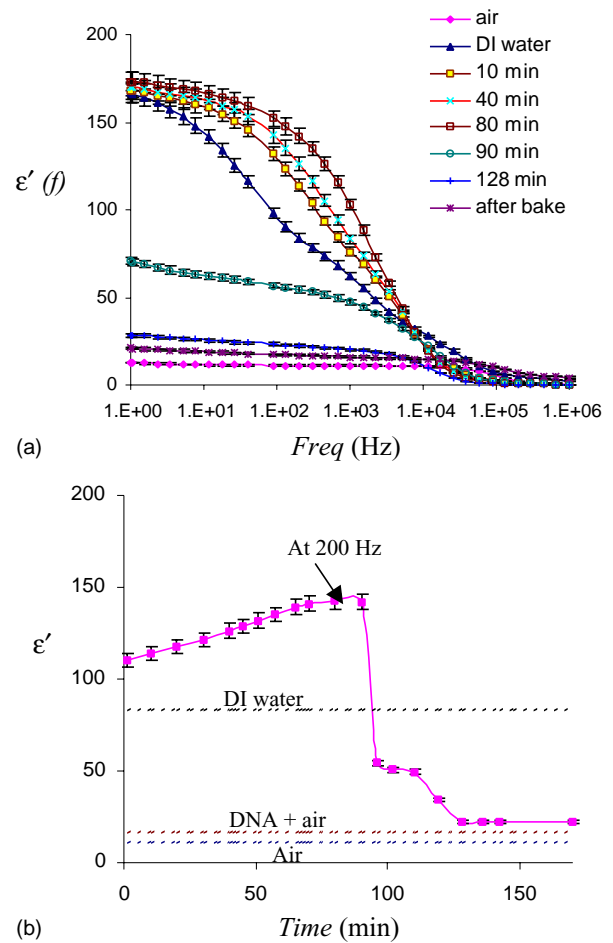


Fig. 5. (a) The dielectric spectroscopy of various concentration DNA solutions inside a 22 nm gap together with the response of the air-filled and DI water-filled gap. Twenty five microliter of $0.5 \mu\text{M}$ target molecular/DI water solution was initially introduced. The DNA concentration increased due to the evaporation. The capacitance of the DNA solution was twice of DI water's around 100 Hz. The capacitance of the dehydrated device was 50% higher than it is originally in air and confirmed that DNA did enter the gap by diffusion. (b) The measured permittivity as a function of time at 200 Hz. Three base lines show the permittivity of air, DI water, and air with DNA after the baking inside the gap, respectively. The permittivity of DNA solution was about twice of water, showing the nanogap's ability in detecting DNA's in solution ($0.5 \mu\text{M}$). A 30% permittivity change due to DNA concentration change was also observed.

slightly (within 5%) for ionic strength smaller than 10^{-3} M ($S_n \leq 1$). As the frequency decreased, the measured permittivity became closer to the theoretical predictions for steady state, showing the theoretical solution as the limit when frequency approaches 0.

Fig. 5a shows the dielectric spectroscopy of DNA solutions inside a 22 nm gap. First, we measured the capacitance of the air-filled and DI water-filled gap, respectively. Then we removed the DI water from the well using a small strip of absorbent paper and added $25 \mu\text{l}$ of $0.5 \mu\text{M}$ target molecular/DI water solution. The well was open to the atmosphere and the DNA concentration increased due to the water evaporation. The dielectric response of the sample

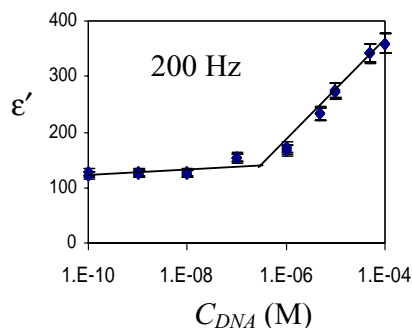


Fig. 6. Permittivity of an aqueous 20-mer ssDNA filled $20 \text{ nm} \times (10)1.5 \mu\text{m} \times 4 \text{ mm}$ gap as a function of the DNA concentration. Capacitance increase due to DNA becomes significant at 100 nM, or about 7×10^4 molecules inside the gap.

solution was measured as a function of time (about one sweep each 5 min). The existence of the DNA was apparent from the capacitance increase in the 100 Hz range from DI water to DNA solution. At 10 min, it was apparent that the capacitance in the gap increased due to the addition of this solution. Subsequent measurements, both at 40 and 80 min, showed an increasing trend in capacitance. By 90 min, however, the capacitance of the gap drastically dropped, to a level lower than that of even DI water alone. This was most likely due to the fact that much of the solution had evaporated and air reentered the gap by this point. A measurement at 128 min and then one after baking further confirmed the evaporation of solution. After dehydrating by baking, the capacitance resembled that of the gap with only air. However, the capacitance increased 50% from the capacitance of gap initially in air. This confirmed that the DNA did enter the gap. Fig. 5b depicts the measured permittivity as a function of time at 200 Hz. Three base lines show the permittivity for gap initially with air, with DI water, and with DNA inside after the baking, respectively. The capacitance filled with DNA solution was about twice of that in water, showing the nanogap sensor's capability in detecting DNA's existence in solution (0.5 μM). A 30% capacitance change due to DNA concentration change was also observed.

The sensitivity of a $20 \text{ nm} \times (10)1.5 \mu\text{m} \times 4 \text{ mm}$ gap in detecting the existence of the target molecule was tested. The gap volume was about 1.2 pl. One target molecule inside the gap corresponded to a target molecular concentration of 1.4 pM. Since we relied on diffusion to introduce target molecules into the gap, there was no guarantee that we could introduce one single molecular into the gap. But we did detect capacitance differences between DI water and the 100 nM target molecular solution (about 70,000 target molecules inside gap at equilibrium). Fig. 6 shows the measured permittivity as a function of DNA concentration at 200 Hz. The capacitance filled with 100 nM target molecular solution was about 4.1 nF (or $\epsilon' \sim 150$) and increased to 9.5 nF (or $\epsilon' \sim 360$) as the target molecular concentration increased to 100 μM while the DI water filled gap had a capacitance of 3.5 nF (or $\epsilon' \sim 130$).

5. Conclusions

The potential to use nanogap capacitors as biomolecular sensors was studied and demonstrated. The electrical charge density and electrical field within the electrolyte-filled nanogap electrodes are obtained by solving the Poisson–Boltzmann equation and the capacitance of the nanogap was then calculated. When the gap size is smaller than the EDL thickness, the potential on the electrode surface decreases as the ionic strength decreases while the potential in the middle of the gap increases. This reduces the potential difference and increases the capacitance. On the other side, the accumulated charge decreases and reduces the capacitance. The result of these two competing effects causes the capacitance to be essentially independent of the ionic strength. The effects of the EDL are that the effective permittivity is proportional to the permittivity of sample solution within the nanogap ($(\epsilon_e/\epsilon) \sim 2.3$). The measured capacitance of a 22 nm gap filled with various ionic strength electrolytes confirms our theoretical prediction.

The dielectric response of target molecules in DI water was measured using a 22 nm gap. The sensitivity of a $20 \text{ nm} \times (10)1.5 \mu\text{m} \times 4 \text{ mm}$ gap in detecting the existence of the target molecules was tested. A capacitance change from 3.5 to 4.1 nF at 200 Hz was recorded between DI water and a 100 nM target molecules solution (about 70,000 molecules inside the gap for equilibrium state). Future work will be determining DNA hybridization events by capacitance change.

Acknowledgements

This work was supported by NSF and DARPA. The devices used in this paper were fabricated in the Berkeley Microfab at the University of California, Berkeley.

References

- Baker-Jarvis, J., Jones, C.A., Riddle, B., 1998. Electrical properties and dielectric relaxation of DNA in solution. NIST Technical Note, 1509.
- Basu, S., Sharma, M.M., 1994. Effect of dielectric saturation on disjoining pressure in thin-films of aqueous-electrolytes. *J. Colloid Interface Sci.* 165, 355–366.
- Biesheuvel, P.M., 2001a. Implications of the charge regulation model for the interaction of hydrophilic surfaces in water. *Langmuir* 17, 3553–3556.
- Biesheuvel, P.M., 2001b. Simplifications of the Poisson–Boltzmann equation for the electrostatic interaction of close hydrophilic surfaces in water. *J. Colloid Interface Sci.* 238, 362–370.
- Chapman, D.L., 1913. A contribution to the theory of electrocapillarity. *Philos. Mag.* 25, 475–481.
- Gouy, G., 1910. Sur la constitution de la charge électrique à la surface d'un électrolyte. *J. Phys. Radium* 9, 457–468.
- Hunter, R.J., 1993. *Introduction to Modern Colloid Science*, Oxford University Press Inc., New York.
- Lee, J.S., Choi, Y.K., Pio, M., Seo, J.G., Lee, L.P., 2002. Nanogap capacitors for label free DNA analysis. *Mat. Res. Soc. Proc.* 729, 185.

- Mandel, M., 1977. Dielectric properties of charged linear macromolecules with particular reference to DNA. *Ann. NY Acad. Sci.* 303, 74–87.
- Marrazza, G., Chianella, I., Mascini, M., 1999. Disposable DNA electrochemical sensor for hybridization detection. *Biosens. Bioelectron.* 14, 43–51.
- Okahata, Y., Kawase, M., Niikura, K., Ohtake, F., Furusawa, H., Ebara, Y., 1998. Kinetic measurements of DNA hybridisation on an oligonucleotide-immobilised 27-MHz quartz crystal microbalance. *Anal. Chem.* 10, 1288–1296.
- Palecek, E., Fojta, M., Tomschik, M., Wang, J., 1998. Electrochemical biosensors for DNA hybridization and DNA damage. *Biosens. Bioelectron.* 13, 621–628.
- Piunno, P.A.E., Krull, U.J., Hudson, R.H.E., Damha, M.J., Cohen, H., 1994. Fiber optic biosensor for fluorometric detection of DNA hybridization. *Anal. Chim. Acta* 288, 205–214.
- Saif, B., Mohr, R.K., Montrose, C.J., Litovitz, T.A., 1991. On the mechanism of dielectric-relaxation in aqueous DNA solutions. *Biopolymers* 31, 1171–1180.
- Sebaek, O., Lee, J.S., Jeong, K.H., Lee, L.P., 2003. Minimization of electrode polarization effect by nanogap electrodes for biosensor applications. *Proceeding 16th IEEE International Micro Electro Mechanical Systems 2003.* 52.
- Takashima, S., 1963. Dielectric dispersion of DNA. *J. Mol. Biol.* 6, 455–467.
- Takashima, S., 1966. Dielectric dispersion of deoxyribonucleic acid 2. *J. Phys. Chem.* 70, 1372.
- Takashima, S., 1967. Effect of ions on dielectric relaxation of DNA. *Biopolymers* 5, 899.
- van der Touw, F., Mandel, M., 1974. Dielectric increment and dielectric-dispersion of solutions containing simple charged linear macromolecules 1. Theory. *Biophys. Chem.* 2, 218–230.
- Zhang, H., Tan, H., Wang, R., Wei, W., Yao, S., 1998. Immobilisation of DNA on silver surface of bulk acoustic wave sensor and its application to the study of UV-C damage. *Anal. Chim. Acta* 374, 31–38.
- Zhmud, B.V., Meurk, A., Bergström, L., 1998. Evaluation of surface ionization parameters from AFM data. *J. Colloid Interface Sci.* 207, 332–343.